arXiv:1608.04629v1 [cond-mat.quant-gas] 16 Aug 2016

Thermal fluctuations enhanced miscibility of binary condensates in optical lattices

K. Suthar[1,2] and D. Angom[1]

[1]*Physical Research Laboratory, Navrangpura, Ahmedabad-380009, Gujarat, India*
[2]*Indian Institute of Technology, Gandhinagar, Ahmedabad-382424, Gujarat, India*

(Dated: August 17, 2016)

We examine the role of thermal fluctuations in two-species Bose-Einstein condensates confined in quasi-two-dimensional (quasi-2D) optical lattices using the Hartree-Fock-Bogoliubov theory with the Popov approximation. The method, in particular, is ideal to probe the evolution of quasiparticle modes at finite temperatures. Our studies show that the quasiparticle spectrum in the phase-separated domain of the two-species Bose-Einstein condensate has a discontinuity at some critical value of the temperature. Furthermore, the low-lying modes like the slosh mode becomes degenerate at this critical temperature, and this is associated with the transition from the immiscible side-by-side density profile to the miscible phase. Hence, the rotational symmetry of the condensate density profiles are restored, and so is the degeneracy of quasiparticle modes.

PACS numbers: 03.75.Mn, 03.75.Hh, 03.75.Lm, 67.85.Hj

I. INTRODUCTION

Ultracold atoms in an optical lattice offer fascinating prospects to study phenomena in many-body physics associated with strongly correlated systems in a highly controllable environment [1–4]. These systems are recognized as ideal tools to explore new quantum phases [5–7], complex phase-transition [8–11], quantum magnetism [12, 13], quantum information [14] and to simulate transport and magnetic properties of condensed-matter systems [15, 16]. Moreover, the effect of phase separation [17, 18], quantum emulsions and coherence properties [19–21], and multicritical behaviour [22, 23] of the mixtures have been explored in the past decade.

Among the various observations made in the two-species Bose-Einstein condensates (TBECs) of ultracold atomic gases, the most remarkable is the phenomenon of phase separation, and it has been a long-standing topic of interest in chemistry and physics. For repulsive on-site interactions, the transition to the phase-separated domain or immiscibility is characterized by the parameter $\Delta = U_{11}U_{22}/U_{12}^2 - 1$, where U_{11} and U_{22} are the intraspecies on-site interactions and U_{12} is the interspecies on-site interaction. When $\Delta < 0$, an immiscible phase occurs in which, the atoms of species 1 and 2 have relatively strong repulsion, whereas $\Delta \geqslant 0$ implies a miscible phase [24–26]. The presence of an external trapping potential, however, modifies this condition as the trap introduces an additional energy cost for the species to spatially separate [27]. In experiments, the unique feature of phase separation has been successfully observed in TBECs with harmonic trapping potential [28–30]. Previously, in the context of superfluid Helium at zero temperature, the phase separation of the bosonic mixtures of isotopes of different masses has also been predicted in Refs. [31, 32]. The recent experimental realizations of TBECs in optical lattices, either of two different atomic species [33] or two different hyperfine states of same atomic species [34, 35] provides the motivations to study these systems in detail. In recent works, we have examined the miscible-immiscible transition, and the quasiparticle spectra of the TBECs at zero temperature [36, 37]. In other theoretical studies, the finite temperature properties of TBECs have been explorered [38–40]. In continuum or TBECs with harmonic confining potentials alone, we have explorered the suppression of phase separation due to the presence of the thermal fluctuations [41]. However, a theoretical understanding of the finite temperature effects on the topology and the collective excitations of TBECs in optical lattices is yet to be explored. The Bose-Einstein condensation and hence, the coherence in a system of bosons depends on the interplay between various parameters, such as temperature, interaction strength, confinement, and dimensionality [42]. In particular, in the low-dimensional Bose gases, the coherence can only be maintained across the entire spatial extent at a temperature much below the critical temperature. The coherence property has already been observed experimentally [43–47].

With an attention towards this unexplored physics, we study the finite temperature effects of quasi-2D trapped TBECs in optical lattices. In the present work, we address the topological phase transition in the TBECs of two different isotopes of Rb with temperature as a control parameter in the domain $T < T_c$, where T_c is the critical temperature of either of the species of the mixture. We study the evolution of the quasiparticle spectra of TBEC in quasi-2D optical lattices with temperature. For this work, we use Hartree-Fock-Bogoliubov (HFB) formalism with the Popov approximation, and starting from phase-separated domain at zero temperature we vary the temperature. We observe a topological transition of the TBEC at a critical value of the temperature. This transition is accompanied by a discontinuity in the quasiparticle excitation spectrum, and in addition, the slosh mode corresponding to each of the species becomes degenerate. Furthermore, we compute the equal-time first order spatial correlation functions which is the measure of the coherence and phase fluctuations present in the system. It describes off-diagonal long range order which is the defining characteristic of BEC [48]. This is an important theoretical tool to study the many body effects in atomic physics experiments [49, 50]. At finite temperature the decay in the coherence of the TBECs is examined using the first order correlation function.

This paper is organized as follows. In Sec. II we describe the HFB-formalism, and the numerical techniques used in the

present work. The evolution of the quasiparticle modes and the density distributions with the temperature are shown in Sec. III. Finally, our main results are summarized in Sec. IV.

II. THEORY AND METHODS

A. HFB-Popov approximation for quasi-2D TBEC

We consider a binary BEC confined in an optical lattice with pancake shaped configuration of background harmonic trapping potential. Thus, the trapping frequencies satisfy the condition $\omega_\perp \ll \omega_z$ with $\omega_x = \omega_y = \omega_\perp$. In this system, the excitation energies along the axial direction is high, and the degree of freedom in this direction is frozen. The excitations, both the quantum and thermal fluctuations, are considered only along the radial direction. In the tight-binding approximation (TBA) [51, 52], the Bose-Hubbard (BH) Hamiltonian [53–55] describing this system is

$$\hat{H} = \sum_{k=1}^{2}\Big[-J_k\sum_{\langle\xi\xi'\rangle}\hat{a}^\dagger_{k\xi}\hat{a}_{k\xi'} + \sum_{\xi}(\epsilon^{(k)}_\xi - \mu_k)\hat{a}^\dagger_{k\xi}\hat{a}_{k\xi}\Big] + \frac{1}{2}\sum_{k=1,\xi}^{2}U_{kk}\hat{a}^\dagger_{k\xi}\hat{a}^\dagger_{k\xi}\hat{a}_{k\xi}\hat{a}_{k\xi} + U_{12}\sum_{\xi}\hat{a}^\dagger_{1\xi}\hat{a}_{1\xi}\hat{a}^\dagger_{2\xi}\hat{a}_{2\xi}, \quad (1)$$

where $k = 1, 2$ is the species index, μ_k is the chemical potential of the kth species, and $\hat{a}_{k\xi}$ ($\hat{a}^\dagger_{k\xi}$) is the annihilation (creation) operators of the two different species at ξth lattice site. The index is such that $\xi \equiv (i, j)$ with i and j as the lattice site index along x and y directions, respectively. The summation index $\langle\xi\xi'\rangle$ represents the sum over nearest-neighbour to ξth site. The TBA is valid when the depth of the lattice potential is much larger than the chemical potential $V_0 \gg \mu_k$, the BH Hamiltonian then describes the system when the bosonic atoms occupy the lowest energy band. A detailed derivation of the BH-Hamiltonian is given in our previous works [36, 37]. In the BH-Hamiltonian, J_k are the tunneling matrix elements, $\epsilon^{(k)}_\xi$ is the offset energy arising due to background harmonic potential, U_{kk} (U_{12}) are the intraspecies (interspecies) interaction strengths. In the present work all the interaction strengths are considered to be repulsive, that is, $U_{kk}, U_{12} > 0$.

In the weakly interacting regime, under the Bogoliubov approximation [56, 57], the annihilation operators at each lattice site can be decomposed as $\hat{a}_{1\xi} = (c_\xi + \hat{\varphi}_{1\xi})e^{-i\mu_1 t/\hbar}$, $\hat{a}_{2\xi} = (d_\xi + \hat{\varphi}_{2\xi})e^{-i\mu_2 t/\hbar}$, where c_ξ and d_ξ are the complex amplitudes describing the condensate phase of each of the species. The operators $\hat{\varphi}_{1\xi}$ and $\hat{\varphi}_{2\xi}$ are the operators representing the quantum or thermal fluctuation part of the field operators. From the equation of motion of the field operators with the Bogoliubov approximation, the equilibrium properties of a TBEC is governed by the coupled generalized discrete nonlinear Schrödinger equations (DNLSEs)

$$\mu_1 c_\xi = -J_1\sum_{\xi'}c_{\xi'} + \Big[\epsilon^{(1)}_\xi + U_{11}(n^c_{1\xi} + 2\tilde{n}_{1\xi}) + U_{12}n_{2\xi}\Big]c_\xi, \quad (2a)$$

$$\mu_2 d_\xi = -J_2\sum_{\xi'}d_{\xi'} + \Big[\epsilon^{(2)}_\xi + U_{22}(n^c_{2\xi} + 2\tilde{n}_{2\xi}) + U_{12}n_{1\xi}\Big]d_\xi, \quad (2b)$$

where $n^c_{1\xi} = |c_\xi|^2$ and $n^c_{2\xi} = |d_\xi|^2$ are the condensate, $\tilde{n}_{k\xi} = \langle\hat{\varphi}^\dagger_{k\xi}\hat{\varphi}_{k\xi}\rangle$ are the noncondensate and $n_{k\xi} = n^c_{k\xi} + \tilde{n}_{k\xi}$ are the total density of the species. Using Bogoliubov transformation

$$\hat{\varphi}_{k\xi} = \sum_l\Big[u^l_{k\xi}\hat{\alpha}_l e^{-i\omega_l t} - v^{*l}_{k\xi}\hat{\alpha}^\dagger_l e^{i\omega_l t}\Big], \quad (3)$$

where $\hat{\alpha}_l(\hat{\alpha}^\dagger_l)$ are the quasiparticle annihilation (creation) operators, which satisfy the Bose commutation relations, l is the quasiparticle mode index, $u^l_{k\xi}$ and $v^l_{k\xi}$ are the quasiparticle amplitudes for the kth species, and $\omega_l = E_l/\hbar$ is the frequency of the lth quasiparticle mode with E_l is the mode excitation energy.

Using the Bogoliubov transformation, we obtain the following HFB-Popov equations [37]:

$$E_l u^l_{1,\xi} = -J_1(u^l_{1,\xi-1} + u^l_{1,\xi+1}) + \mathcal{U}_1 u^l_{1,\xi} - U_{11}c^2_\xi v^l_{1,\xi} + U_{12}c_\xi(d^*_\xi u^l_{2,\xi} - d_\xi v^l_{2,\xi}), \quad (4a)$$

$$E_l v^l_{1,\xi} = J_1(v^l_{1,\xi-1} + v^l_{1,\xi+1}) + \underline{\mathcal{U}}_1 v^l_{1,\xi} + U_{11}c^{*2}_\xi u^l_{1,\xi} - U_{12}c^*_\xi(d_\xi v^l_{2,\xi} - d^*_\xi u^l_{2,\xi}), \quad (4b)$$

$$E_l u^l_{2,\xi} = -J_2(u^l_{2,\xi-1} + u^l_{2,\xi+1}) + \mathcal{U}_2 u^l_{2,\xi} - U_{22}d^2_\xi v^l_{2,\xi} + U_{12}d_\xi(c^*_\xi u^l_{1,\xi} - c_\xi v^l_{1,\xi}), \quad (4c)$$

$$E_l v^l_{2,\xi} = J_2(v^l_{2,\xi-1} + v^l_{2,\xi+1}) + \underline{\mathcal{U}}_2 v^l_{2,\xi} + U_{22}d^{*2}_\xi u^l_{2,\xi} - U_{12}d^*_\xi(c_\xi v^l_{1,\xi} - c^*_\xi u^l_{1,\xi}), \quad (4d)$$

where $\mathcal{U}_1 = 2U_{11}(n^c_{1\xi} + \tilde{n}_{1\xi}) + U_{12}(n^c_{2\xi} + \tilde{n}_{2\xi}) + (\epsilon^{(1)}_\xi - \mu_1)$, $\mathcal{U}_2 = 2U_{22}(n^c_{2\xi} + \tilde{n}_{2\xi}) + U_{12}(n^c_{1\xi} + \tilde{n}_{1\xi}) + (\epsilon^{(2)}_\xi - \mu_2)$ with $\underline{\mathcal{U}}_k = -\mathcal{U}_k$. To solve the above eigenvalue equations, we use a basis set of on-site Gaussian wave functions, and define the quasiparticle amplitude as linear combination of the basis functions. The condensate and noncondensate densities are then computed through the self-consistent solution of Eqs. (2) and (4). The noncondensate atomic density at the ξth lattice site is

$$\tilde{n}_{k\xi} = \sum_l\left[(|u^l_{k\xi}|^2 + |v^l_{k\xi}|^2)N_0(E_l) + |v^l_{k\xi}|^2\right], \quad (5)$$

where $N_0(E_l) = (e^{\beta E_l} - 1)^{-1}$ with $\beta = (k_B T)^{-1}$ is the Bose-Einstein distribution factor of the lth quasiparticle mode with energy E_l at temperature T. The last term in the $\tilde{n}_{k\xi}$ is independent of the temperature, and hence, represents the quantum fluctuations of the system. To examine the role of temperature we measure the miscibility of the condensates in

terms of the overlap integral

$$\Lambda = \frac{\left[\int n_1(\mathbf{r}) n_2(\mathbf{r}) d\mathbf{r}\right]^2}{\left[\int n_1^2(\mathbf{r}) d\mathbf{r}\right]\left[\int n_2^2(\mathbf{r}) d\mathbf{r}\right]}. \tag{6}$$

Here $n_k(\mathbf{r})$ is the total density of kth condensate at position $\mathbf{r} \equiv (x, y)$. If the two condensate of the TBEC complete overlap to each other then the system is in miscible phase with $\Lambda = 1$, whereas for the completely phase-separated case $\Lambda = 0$.

B. Field-field correlation function

To define a measure of the coherence in the condensate we introduce the first order correlation function $g_k^{(1)}(\mathbf{r}, \mathbf{r}')$, which can be expressed as expectations of product of field operators at different positions and times [58–61]. These are normalized to attain unit modulus in the case of perfect coherence. Here, we restrict ourselves to discussing ordered spatial correlation functions at a fixed time. In terms of the quantum Bose field operator $\hat{\Psi}_k$ the first-order spatial correlation function is

$$g_k^{(1)}(\mathbf{r}, \mathbf{r}') = \frac{\langle \hat{\Psi}_k^\dagger(\mathbf{r}) \hat{\Psi}_k(\mathbf{r}') \rangle}{\sqrt{\langle \hat{\Psi}_k^\dagger(\mathbf{r}) \hat{\Psi}_k(\mathbf{r}) \rangle \langle \hat{\Psi}_k^\dagger(\mathbf{r}') \hat{\Psi}_k(\mathbf{r}') \rangle}}, \tag{7}$$

where, $\langle \cdots \rangle$ represents thermal average. It is important to note that the local first order correlation function is equal to the density, i.e. $g_k^{(1)}(\mathbf{r}, \mathbf{r}) = n_k(\mathbf{r})$. The expression of $g_k^{(1)}(\mathbf{r}, \mathbf{r}')$ can also written in terms of condensate, and non-condensate correlations as

$$g_k^{(1)}(\mathbf{r}, \mathbf{r}') = \frac{n_k^c(\mathbf{r}, \mathbf{r}') + \tilde{n}_k(\mathbf{r}, \mathbf{r}')}{\sqrt{n_k(\mathbf{r}) n_k(\mathbf{r}')}}, \tag{8}$$

where,

$$\begin{aligned} n_k^c(\mathbf{r}, \mathbf{r}') &= \psi_k^*(\mathbf{r}) \psi_k(\mathbf{r}'), \\ \tilde{n}_k(\mathbf{r}, \mathbf{r}') &= \sum_l \big[\left\{ u_k^{*l}(\mathbf{r}) u_k^l(\mathbf{r}') + v_k^{*l}(\mathbf{r}) v_k^l(\mathbf{r}') \right\} N_0(E_l) \\ &\quad + v_k^{*l}(\mathbf{r}) v_k^l(\mathbf{r}') \big], \\ n_k(\mathbf{r}) &= n_k^c(\mathbf{r}) + \tilde{n}_k(\mathbf{r}) \end{aligned}$$

are the condensate density correlation, noncondensate correlation and total density of the kth species, respectively. In the above expressions the $n_k^c(\mathbf{r}, \mathbf{r}')$ and $\tilde{n}_k(\mathbf{r}, \mathbf{r}')$ are obtained by expanding the complex amplitudes (c_ξ, d_ξ) and the quasiparticle amplitudes $(u_{k,\xi}^l, v_{k,\xi}^l)$ in the localized Gaussian basis. At $T = 0$ K, the entire condensate cloud has complete coherence, and therefore $g^{(1)} = 1$ within the condensate region. In TBECs, the transition from phase-separated to the miscible domain at $T \neq 0$ is characteristic signature in the spatial structure of $g_k^{(1)}(\mathbf{r}, \mathbf{r}')$.

C. Numerical methods

To solve the coupled DNLSEs, Eqs. (2), we scale and rewrite the equations in the dimensionless form. For this we choose the characteristic length scale as the lattice constant $a = \lambda_L/2$ with λ_L as the wavelength of the laser which creates the lattice potential. Similarly, the recoil energy $E_R = \hbar^2 k_L^2/2m$ with $k_L = 2\pi/\lambda_L$ is chosen as the energy scale of the system. We use fourth order Runge-Kutta method to solve these equations for zero as well as finite temperatures. To start the iterative steps to solve the equations an appropriate initial guess value of c_ξ and d_ξ are chosen. For the present work we chose the values corresponding to the side-by-side profile as it gives quasiparticle excitation energies which are real, and not complex. This is important as this shows that the solution we obtain is a stable one, and not metastable. The stationary ground-state wave-function of the TBEC is obtained through imaginary time propagation. In the tight-binding limit, the width of the orthonormalized Gaussian basis functions localized at each lattice site is $0.3a$. Furthermore, to study the quasiparticle excitation spectrum, we cast Eqs. (4) as matrix eigenvalue equations and diagonalize the matrix using the routine ZGEEV from the LAPACK library [62]. For finite temperature computations, to take into account the thermal fluctuations, we solve the coupled equations Eqs. (2) and Eqs. (4) self-consistently. The solution of the DNLSEs is iterated until it satisfies the convergence criteria in terms of the number of condensate and noncondensate atoms. In general, the convergence is not smooth, and most of the time we encounter severe oscillations in the number of atoms. To remedy these oscillations by damping, we use a successive over- (under-) relaxation technique while updating the condensate (noncondensate) atoms. The new solutions after an iteration cycle (IC) are

$$c_{\xi,\mathrm{IC}}^{\mathrm{new}} = r^{\mathrm{ov}} c_{\xi,\mathrm{IC}} + (1 - r^{\mathrm{ov}}) c_{\xi,\mathrm{IC}-1}, \tag{9a}$$

$$d_{\xi,\mathrm{IC}}^{\mathrm{new}} = r^{\mathrm{ov}} d_{\xi,\mathrm{IC}} + (1 - r^{\mathrm{ov}}) d_{\xi,\mathrm{IC}-1}, \tag{9b}$$

$$\tilde{n}_{k\xi,\mathrm{IC}}^{\mathrm{new}} = r^{\mathrm{un}} \tilde{n}_{k\xi,\mathrm{IC}} + (1 - r^{\mathrm{un}}) \tilde{n}_{k\xi,\mathrm{IC}-1}, \tag{9c}$$

where $r^{\mathrm{ov}} > 1$ ($r^{\mathrm{un}} < 1$) is the over (under) relaxation parameter.

III. RESULTS AND DISCUSSIONS

To examine the effects of thermal fluctuations on the quasiparticle spectra we consider the ^{87}Rb -^{85}Rb TBEC with ^{87}Rb labeled as species 1 and ^{85}Rb labeled as species 2. The radial trapping frequencies of the harmonic potential are $\omega_x = \omega_y = 2\pi \times 50$ Hz with the anisotropy parameter $\omega_z/\omega_\perp = 20.33$, and these parameters are chosen on the experimental work Gadway and collaborators [34]. It is important to note that we consider equal background trapping potential for species 1 and 2. The laser wavelength used to create the 2D lattice potential and the lattice depth are $\lambda_L = 1064$ nm and $V_0 = 5E_R$, respectively. We then take the total number of atoms $N_1 = N_2 = 100$ confined in a (40×40) quasi-2D lattice system. It must be mentioned that, the number of lat-

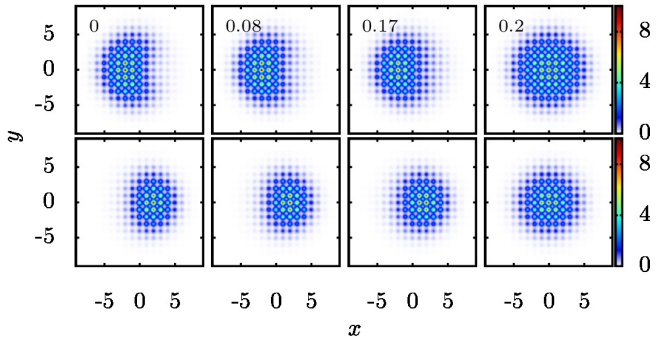

FIG. 1. The condensate density profiles at different temperatures in phase-separated domain of ^{87}Rb -^{85}Rb TBEC. The condensate density distribution of the first species (upper panel) and the second species (lower panel) are shown at $T/T_c = 0, 0.08, 0.17$, and 0.2, which correspond to $T = 0, 30, 60$, and 70 nK. Here x and y are measured in units of the lattice constant a.

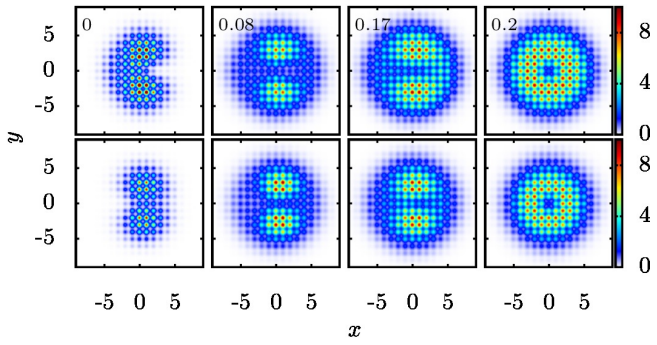

FIG. 2. The noncondensate density profile at different temperatures in phase-separated domain of ^{87}Rb -^{85}Rb TBEC. The density distribution of the noncondensate atoms of first species (upper panel) and the second species (lower panel) are shown at $T/T_c = 0, 0.08, 0.17$, and 0.2, which correspond to $T = 0, 30, 60$, and 70 nK. Here x and y are measured in units of the lattice constant a.

tice sites considered much larger than the spatial extent of the condensate cloud. Albeit the computations are more time consuming with the larger lattice size, we chose it to ensure that the spatial extent of the thermal component is confined well within the lattice considered. The tunneling matrix elements are $J_1 = 0.66E_R$ and $J_2 = 0.71E_R$, which correspond to an optical lattice potential with a depth of $5E_R$. The intraspecies and interspecies on-site interactions are set as $U_{11} = 0.07E_R$, $U_{22} = 0.02E_R$ and $U_{12} = 0.15E_R$, respectively. For this set of parameters the ground state density distribution of ^{87}Rb -^{85}Rb TBEC is phase-separated with side-by-side geometry. This is a symmetry-broken profile where one species is placed to the left and other to the right of trap center along y-axis. The evolution of the ground state from miscible to the side-by-side density profile due to decrease in the U_{22} is reported in our previous work [37]. In the present work, we demonstrate the role of temperature in the phase-separated domain of the binary condensate.

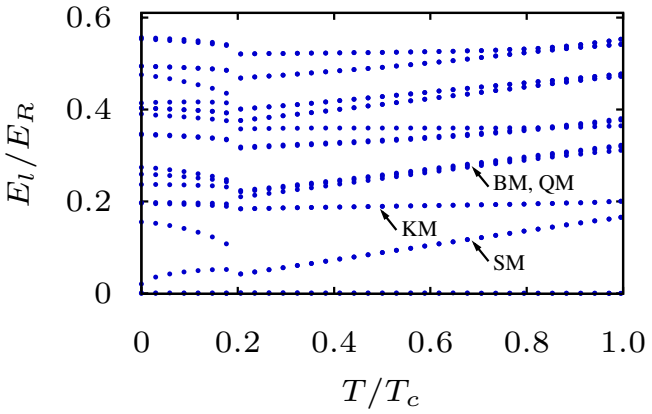

FIG. 3. The quasiparticle energies of the low-lying modes as a function of the temperature in phase-separated domain of ^{87}Rb -^{85}Rb TBEC. At $T/T_c = 0.185$ the Kohn and higher modes energy becomes degenerate and system transformed from side-by-side to miscible density profile. In the figure, the slosh mode (SM), Kohn mode (KM), breathing mode (BM), and quadrupole mode (QM) are marked by the black arrows. Here the excitation energy E_l and the temperature T are scaled with respect to the recoil energy E_R and the critical temperature T_c of ^{87}Rb.

A. Zero temperature

At $T = 0$ K, in the phase-separated domain, the energetically preferable ground state of TBEC is the side-by-side geometry, which is reported in our previous work [37]. Unlike in one-dimensional system [36] in quasi-2D system the presence of the quantum fluctuations does not alter the ground state. We start with the phase-separated ^{87}Rb -^{85}Rb TBEC, which has the overlap integral $\Lambda = 0.10$. The density distributions of the condensate and noncondensate atoms of the two species at $T = 0$ K is shown in Fig. 1 and Fig. 2. This is a symmetry broken side-by-side geometry with noncondensate atoms more localized at the edges of the condensate along y-axis.

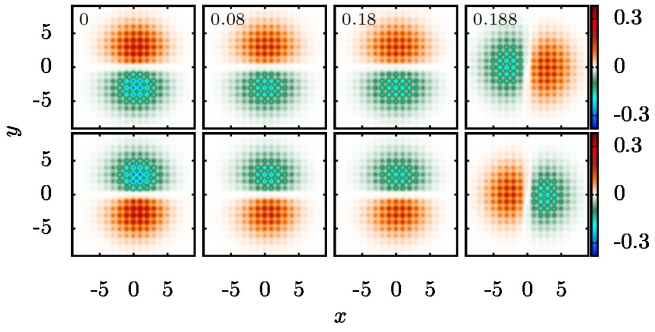

FIG. 4. The mode function of first excitation mode (slosh mode) as a function of the temperature in phase-separated domain of ^{87}Rb -^{85}Rb TBEC. The slosh mode is an out-of-phase mode, where the density flow of first species (upper pannel) is in opposite direction to the flow of second species (lower panel). The value of T/T_c is shown at the upper left corner of each plot in upper panel. These values correspond to $T = 0, 30, 64$, and 66 nK. Here x and y are in units of the lattice constant a.

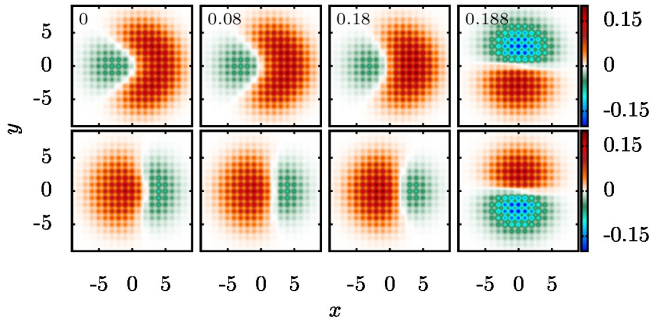

FIG. 5. The mode function of second excitation mode (slosh mode), which at $T/T_c > 0.185$ becomes degenerate to the mode shown in Fig. 4 of ^{87}Rb -^{85}Rb TBEC. Here the density flow of first species (upper panel) is out of phase to the flow of second species (lower panel). The value of T/T_c is shown at the upper left corner of each plot in upper panel. These values correspond to $T = 0, 30, 64$, and 66 nK. Here x and y are in units of the lattice constant a.

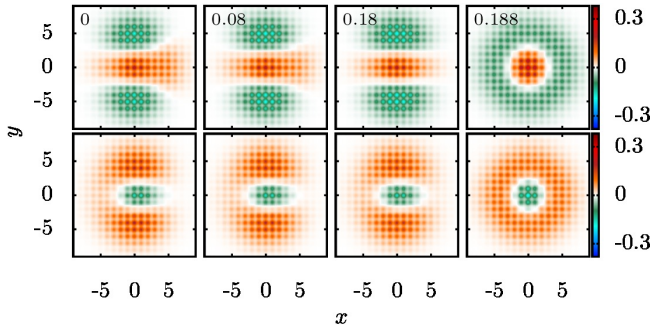

FIG. 6. The evolution of the interface mode in the phase-separated domain of ^{87}Rb -^{85}Rb TBEC with temperature. At $T/T_c > 0.185$, this mode transformed into breathing mode as the system acquires the rotational symmetry. These are out-of-phase modes as the density perturbation of first species (upper panel) is in opposite direction to the second species (lower panel). The value of T/T_c is shown at the upper left corner of each plot in upper panel. Here x and y are in units of the lattice constant a.

B. Finite temperatures

At $T \neq 0$, in addition to the quantum fluctuations, which are present at the zero temperature, the thermal cloud also contribute to the noncondensate density. As shown in Figs. 1 and 2, at $T = 30$ nK, the condensate density profiles of both the species begin to overlap, or in other words, the two species are partly miscible. This is also evident from the value of $\Lambda = 0.16$, which shows a marginal increase compared to value of 0.10 at zero temperature. Upon further increase in temperature, at $T = 60$ nK, $\Lambda = 0.36$, this indicates an increase in the miscibility of the two species. Another important feature at 30 and 60 nK is the localization of the noncondensate atoms at the interface. This is due to repulsion from the condensate atoms, and lower thermal energy which is insufficient to overcome this repulsion energy. At higher temperatures, the extent of overlap between the condensate density profiles increases, and TBEC is completely miscible at $T = 70$ nK. This is reflected in the value of $\Lambda = 0.95$, and the condensate as well as the noncondensate densities acquire rotational symmetry.

The transition from the phase-separated into miscible domain can further be examined from the evolution of the quasiparticle modes as a function of the temperature. The evolution of the few low-lying mode energies with temperature is shown in Fig. 3 with the temperature defined in the units of the critical temperature T_c of the ^{87}Rb atoms. It is evident from the figure that there are mode energy bifurcations with the increase in the temperature. These are associated with the restoration of rotational symmetry when the TBEC is rendered miscible through an increase in temperature.

As to be expected the two lowest energy mode are the zero energy or the Goldstone modes, which are the result of the spontaneous symmetry breaking associated with the condensation. In the phase-separated domain, these modes correspond to one each for each of the species. The first two excited modes are the non-degenerate Kohn or slosh modes of the two species, and these remain non-degenerate in the domain $T/T_c \leq 0.185$. The structure of these modes are shown in Figs. 4 and 5. When $T/T_c > 0.185$ the TBEC acquires a rotational symmetry and the slosh modes becomes degenerate with $\pi/2$ rotation. A key feature in the quasiparticle mode evolution is that the energy of all the out-of-phase mode increases for $T/T_c > 0.185$, whereas all the in-phase mode remains steady. Here, out-of-phase and in-phase mean the amplitudes u_1 and u_2 of a quasiparticle are of different and same phases, respectively. Among the low-energy modes, the Kohn mode is an in-phase whereas the breathing and quadrupole modes are out of phase in nature. One unique feature of TBEC in the immiscible phase is the presence of interface modes, which have amplitudes prominent around the interface region. The existence of these modes is reported in our previous work [37], and were investigated in other works [63, 64] for TBECs confined in harmonic potential alone at zero temperature. One of the low-energy interface modes is shown in Fig. 6. It is evident from the figure that the mode is out-of-phase in nature, and it is transformed into breathing mode of the miscible domain when $T/T_c > 0.185$. In the miscible domain, the breathing mode becomes degenerate with the quadrupole mode and gain energy. The quasiparticles of the miscible domain have well-defined azimuthal quantum number, and modes undergo rotations as T is further increased.

To investigate the spatial coherence of TBEC at equilibrium, we examine the trends in $g_k^{(1)}(0, \mathbf{r})$ defined earlier in Eq. (8), and are shown in Fig. 7 for various temperatures. As mentioned earlier, at $T = 0$ K, $n_k(\mathbf{r}) \approx n_k^c(\mathbf{r})$ have complete phase coherence, and therefore, $g_k^{(1)} = 1$ within the extent of the condensates, this is shown in Fig. 7. At zero temperature or in the limit $\tilde{n}_k \equiv 0$ the correlation function, Eq. (8), resemble a Heaviside function, and the negligible contribution from the quantum fluctuations smooth out the sharp edges as $g_k^{(1)}$ drops to zero. More importantly, in the numerical computations this cause a loss of numerical accuracy as it involves division of two small numbers in Eq. (8) [65]. However at

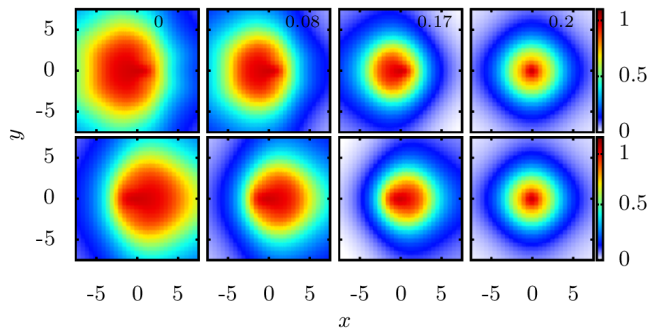

FIG. 7. The first-order off-diagonal correlation function $g_k^{(1)}(0,\mathbf{r})$ of ^{87}Rb (upper panel) and ^{85}Rb (lower panel) at $T/T_c = 0, 0.08, 0.17$, and 0.2, which correspond to $T = 0, 30, 60$, and 70 nK. Here x and y are measured in units of the lattice constant a.

finite temperature the presence of the noncondensate atoms modify the nature of the spatial coherence present in the system. The decay rate of the correlation function increases with the temperature, and this is evident from Fig. 7, which shows $g_k^{(1)}(0,\mathbf{r})$ at $T = 30, 60$, and 70 nK. In addition to this, the transition from phase-separated to the miscible TBEC is also reflected in the decay trends of $g_k^{(1)}(0,\mathbf{r})$.

IV. CONCLUSIONS

We have examined the finite temperature effects on the phenomenon of phase separation in TBECs confined in quasi-2D optical lattices. As temperature is increased the phase-separated side-by-side ground state geometry is transformed into miscible phase. For the case of TBEC comprising of ^{87}Rb and ^{85}Rb, the transformation occurs at $T/T_c \approx 0.185$. This demonstrates the importance of thermal fluctuations which can make TBECs miscible albeit the interaction parameters satisfy the criterion of phase separation. The other key observation is that the transition from phase-separated domain to miscible domain is associated with a change in the nature of the quasiparticle energies. The low-lying out-of-phase mode, in particular, the slosh mode becomes degenerate and increase in energy. On the other hand, the in-phase mode, such as Kohn mode, remain steady as temperature ($T < T_c$) is increased. The interface modes, which are unique to the phase-separated domain, in addition to change in energy are geometrically transformed into rotationally symmetric breathing modes in the miscible domain. The temperature driven immiscible to the miscible transition is also evident in the profile of the correlation functions.

ACKNOWLEDGMENTS

We thank Arko Roy, S. Gautam, S. Bandyopadhyay and R. Bai for useful discussions. The results presented in the paper are based on the computations using Vikram-100, the 100TFLOP HPC Cluster at Physical Research Laboratory, Ahmedabad, India.

[1] D. Jaksch, C. Bruder, J. I. Cirac, C. W. Gardiner, and P. Zoller, Phys. Rev. Lett. **81**, 3108 (1998).
[2] C. Orzel, A. K. Tuchman, M. L. Fenselau, M. Yasuda, and M. A. Kasevich, Science **291**, 2386 (2001).
[3] M. Greiner, O. Mandel, T. Esslinger, T. W. Hansch, and I. Bloch, Nature (London) **415**, 39 (2002).
[4] I. Bloch, J. Dalibard, and S. Nascimbene, Nat. Phys. **8**, 267 (2012).
[5] E. Demler and F. Zhou, Phys. Rev. Lett. **88**, 163001 (2002).
[6] A. B. Kuklov and B. V. Svistunov, Phys. Rev. Lett. **90**, 100401 (2003).
[7] A. Kuklov, N. Prokof'ev, and B. Svistunov, Phys. Rev. Lett. **92**, 050402 (2004).
[8] A. Pal and D. A. Huse, Phys. Rev. B **82**, 174411 (2010).
[9] S. Choi and L. Radzihovsky, Phys. Rev. A **84**, 043612 (2011).
[10] H.-F. Lin, H.-D. Liu, H.-S. Tao, and W.-M. Liu, Sci. Rep. **5**, 9810 (2015).
[11] O. Jrgensen, K. Sengstock, and D.-S. Lhmann, Sci. Rep. **5**, 12912 (2015).
[12] S. Trotzky, P. Cheinet, S. Fölling, M. Feld, U. Schnorrberger, A. M. Rey, A. Polkovnikov, E. A. Demler, M. D. Lukin, and I. Bloch, Science **319**, 295 (2008).
[13] J. Simon, W. S. Bakr, R. Ma, M. E. Tai, P. M. Preiss, and M. Greiner, Nature **472**, 307 (2011).
[14] I. Bloch, Nature **453**, 1016 (2008).
[15] M. Lewenstein, A. Sanpera, V. Ahufinger, B. Damski, A. Sen(De), and U. Sen, Adv. Phys. **56**, 243 (2007).
[16] I. Bloch, J. Dalibard, and W. Zwerger, Rev. Mod. Phys. **80**, 885 (2008).
[17] T. Mishra, R. V. Pai, and B. P. Das, Phys. Rev. A **76**, 013604 (2007).
[18] F. Zhan and I. P. McCulloch, Phys. Rev. A **89**, 057601 (2014).
[19] M. Greiner, I. Bloch, O. Mandel, T. W. Hänsch, and T. Esslinger, Phys. Rev. Lett. **87**, 160405 (2001).
[20] T. Roscilde and J. I. Cirac, Phys. Rev. Lett. **98**, 190402 (2007).
[21] P. Buonsante, S. M. Giampaolo, F. Illuminati, V. Penna, and A. Vezzani, Phys. Rev. Lett. **100**, 240402 (2008).
[22] G. Ceccarelli, J. Nespolo, A. Pelissetto, and E. Vicari, Phys. Rev. A **92**, 043613 (2015).
[23] G. Ceccarelli, J. Nespolo, A. Pelissetto, and E. Vicari, Phys. Rev. A **93**, 033647 (2016).
[24] T.-L. Ho and V. B. Shenoy, Phys. Rev. Lett. **77**, 3276 (1996).
[25] E. Timmermans, Phys. Rev. Lett. **81**, 5718 (1998).
[26] B. D. Esry and C. H. Greene, Phys. Rev. A **59**, 1457 (1999).
[27] L. Wen, W. M. Liu, Y. Cai, J. M. Zhang, and J. Hu, Phys. Rev. A **85**, 043602 (2012).
[28] S. B. Papp, J. M. Pino, and C. E. Wieman, Phys. Rev. Lett. **101**, 040402 (2008).
[29] S. Tojo, Y. Taguchi, Y. Masuyama, T. Hayashi, H. Saito, and T. Hirano, Phys. Rev. A **82**, 033609 (2010).

[30] D. J. McCarron, H. W. Cho, D. L. Jenkin, M. P. Köppinger, and S. L. Cornish, Phys. Rev. A **84**, 011603 (2011).
[31] G. V. Chester, Phys. Rev. **100**, 446 (1955).
[32] M. D. Miller, Phys. Rev. B **18**, 4730 (1978).
[33] J. Catani, L. De Sarlo, G. Barontini, F. Minardi, and M. Inguscio, Phys. Rev. A **77**, 011603 (2008).
[34] B. Gadway, D. Pertot, R. Reimann, and D. Schneble, Phys. Rev. Lett. **105**, 045303 (2010).
[35] P. Soltan-Panahi, J. Struck, P. Hauke, A. Bick, W. Plenkers, G. Meineke, C. Becker, P. Windpassinger, M. Lewenstein, and K. Sengstock, Nat. Phys. **7**, 434 (2011).
[36] K. Suthar, A. Roy, and D. Angom, Phys. Rev. A **91**, 043615 (2015).
[37] K. Suthar and D. Angom, Phys. Rev. A **93**, 063608 (2016).
[38] P. Öhberg, Phys. Rev. A **61**, 013601 (1999).
[39] H. Shi, W.-M. Zheng, and S.-T. Chui, Phys. Rev. A **61**, 063613 (2000).
[40] K. Nho and D. P. Landau, Phys. Rev. A **76**, 053610 (2007).
[41] A. Roy and D. Angom, Phys. Rev. A **92**, 011601 (2015).
[42] N. P. Proukakis, Phys. Rev. A **74**, 053617 (2006).
[43] S. Dettmer, D. Hellweg, P. Ryytty, J. J. Arlt, W. Ertmer, K. Sengstock, D. S. Petrov, G. V. Shlyapnikov, H. Kreutzmann, L. Santos, and M. Lewenstein, Phys. Rev. Lett. **87**, 160406 (2001).
[44] D. Hellweg, L. Cacciapuoti, M. Kottke, T. Schulte, K. Sengstock, W. Ertmer, and J. J. Arlt, Phys. Rev. Lett. **91**, 010406 (2003).
[45] S. Richard, F. Gerbier, J. H. Thywissen, M. Hugbart, P. Bouyer, and A. Aspect, Phys. Rev. Lett. **91**, 010405 (2003).
[46] J. Esteve, J.-B. Trebbia, T. Schumm, A. Aspect, C. I. Westbrook, and I. Bouchoule, Phys. Rev. Lett. **96**, 130403 (2006).
[47] T. Plisson, B. Allard, M. Holzmann, G. Salomon, A. Aspect, P. Bouyer, and T. Bourdel, Phys. Rev. A **84**, 061606 (2011).
[48] O. Penrose and L. Onsager, Phys. Rev. **104**, 576 (1956).
[49] E. A. Burt, R. W. Ghrist, C. J. Myatt, M. J. Holland, E. A. Cornell, and C. E. Wieman, Phys. Rev. Lett. **79**, 337 (1997).
[50] B. L. Tolra, K. M. O'Hara, J. H. Huckans, W. D. Phillips, S. L. Rolston, and J. V. Porto, Phys. Rev. Lett. **92**, 190401 (2004).
[51] M. L. Chiofalo, M. Polini, and M. P. Tosi, Eur. Phys. J. D **11**, 371 (2000).
[52] A. Smerzi and A. Trombettoni, Phys. Rev. A **68**, 023613 (2003).
[53] M. P. A. Fisher, P. B. Weichman, G. Grinstein, and D. S. Fisher, Phys. Rev. B **40**, 546 (1989).
[54] E. Lundh and J.-P. Martikainen, Phys. Rev. A **85**, 023628 (2012).
[55] P. P. Hofer, C. Bruder, and V. M. Stojanović, Phys. Rev. A **86**, 033627 (2012).
[56] A. Griffin, Phys. Rev. B **53**, 9341 (1996).
[57] A. M. Rey, *Ultracold bosonic atoms in optical lattices*, Ph.D. thesis, University of Maryland, USA (2004).
[58] R. J. Glauber, Phys. Rev. **131**, 2766 (1963).
[59] M. Naraschewski and R. J. Glauber, Phys. Rev. A **59**, 4595 (1999).
[60] A. Bezett, E. Toth, and P. B. Blakie, Phys. Rev. A **77**, 023602 (2008).
[61] A. Bezett and E. Lundh, J. Phys. B **45**, 205301 (2012).
[62] E. Anderson, Z. Bai, C. Bischof, S. Blackford, J. Demmel, J. Dongarra, J. D. Croz, A. Greenbaum, S. Hammarling, A. McKenney, and D. Sorensen, *LAPACK Users' Guide*, 3rd ed. (Society for Industrial and Applied Mathematics, Philadelphia, PA, 1999).
[63] C. Ticknor, Phys. Rev. A **88**, 013623 (2013).
[64] C. Ticknor, Phys. Rev. A **89**, 053601 (2014).
[65] C. Gies and D. A. W. Hutchinson, Phys. Rev. A **70**, 043606 (2004).